AIAA JOURNAL
Vol. 48, No. 12, December 2010

New Families of Hygrothermally Stable Composite Laminates with Optimal Extension-Twist Coupling

Robert A. Haynes*
Georgia Institute of Technology, Atlanta, Georgia 30332
and
Erian A. Armanios†
University of Texas at Arlington, Arlington, Texas 76019

DOI: 10.2514/1.J050596

The necessary and sufficient conditions for hygrothermal stability of laminated composites are presented. A thorough survey of hygrothermally stable families is performed to identify stacking sequences that produce maximum extension-twist coupling. This is achieved through a constrained optimization routine, where the objective function is derived from the constitutive law given in classical lamination theory and the constraints are the necessary conditions for hygrothermal stability. A representative sample of these optimized laminates are constructed and tested to demonstrate significant improvement in coupling over the previously known optima. Comparisons are made with a nonlinear model and finite element analysis. An investigation of the robustness of the optimal stacking sequences to errors in ply angle typical of hand-layup manufacturing is presented.

Nomenclature

A_{ij} = in-plane stiffness coefficients
B_{ij} = coupling stiffness coefficients
b_i = coefficients that are functions of A_{ij}, B_{ij}, D_{ij}, and geometric parameters
D_{ij} = bending stiffness coefficients
E_{11} = elastic modulus along the fiber direction
F_a = axial force
h_k = distance of the kth ply measured from the laminate midplane
L = length of a specimen
M_{ij} = out-of-plane stress resultants
N_{ij} = in-plane stress resultants
n = number of plies
$\bar{Q}_{ij(k)}$ = transformed reduced stiffness coefficients of the kth ply
T, H = nonmechanical quantities
t = ply thickness
w = specimen width
α_{ij} = in-plane compliance coefficients
β_{ij} = coupling compliance coefficients
γ_{xy} = in-plane shear strain
δ_{ij} = bending compliance coefficients
ε_{ii} = in-plane extensional strains
η = nondimensional parameter for comparing extension-twist coupling
θ_k = fiber orientation angle of the kth ply
θ_t = twist angle
κ_{ij} = out-of-plane curvatures
σ_o = nominal stress
σ_{xx} = axial stress
φ = twist rate
φ_{oL} = tip pretwist angle
φ_L = tip twist angle

Presented as Paper 2010-2773 at the 51st AIAA/ASME/ASCE/AHS/ASC Structures, Structural Dynamics, and Materials Conference, Orlando, FL, 12–15 April 2010; received 6 April 2010; revision received 12 August 2010; accepted for publication 17 August 2010.

*Graduate Research Assistant, School of Aerospace Engineering, 270 Ferst Dr. NW. Member AIAA.

†Professor and Chair, Mechanical and Aerospace Engineering Department, Box 19018, 500 W. First Street, Woolf Hall 211. Associate Fellow AIAA.

I. Introduction

LAMINATED composite materials can be tailored through judicious alignment of the fibers of each constituent ply to produce an advantageous structural response beyond what is achievable with conventional materials. For example, extension-twist coupling has applications in rotor blades to passively adjust the blade twist distribution with a change in rotor speed. Specifically, this concept could be used to mitigate the effects of a gust on a wind turbine or achieve optimum propulsive efficiency on a tilt-rotor aircraft in both vertical and forward flight regimes.

A symmetric stacking sequence precludes any coupling between in-plane and out-of-plane deformation modes; therefore, an asymmetric stacking sequence is necessary to achieve extension-twist coupling in a flat laminate. The simplest way to achieve extension-twist coupling is with an angle-ply stacking sequence, i.e. $[\pm\theta]$, where θ is the fiber-orientation angle. Asymmetric stacking sequences, such as angle-ply, are often *hygrothermally unstable* [1,2], meaning they warp out-of-plane with changes in temperature or moisture. The laminate defined by $[0/90]_s$ is hygrothermally isotropic, meaning it has equal hygrothermal expansion in all directions. Winckler [3] first reported combining angle-ply and hygrothermally isotropic laminates to create a stacking sequence that is *hygrothermally stable* but still retains extension-twist coupling. The original stacking sequence is given by

$$[\theta/(\theta-90)_2/\theta/-\theta/(90-\theta)_2/-\theta] \tag{1}$$

While intuitive, the laminate described by Eq. (1) has not been shown to be unique or optimal. In fact, the present work demonstrates that not only are there other hygrothermally stable laminates, some can be demonstrated to have significantly more extension-twist coupling than the Winckler-type laminates. This is shown by first establishing the necessary and sufficient conditions for hygrothermal stability. Next, using these conditions, a constrained optimization is performed to maximize the parameter that represents the level of extension-twist coupling achievable for a given number of plies. These optimized laminates are constructed, tested, and verified to have improved extension-twist coupling. Predictions from a geometrically nonlinear model and finite element analysis are confirmed by comparison with test results.

II. Necessary and Sufficient Conditions for Hygrothermal Stability

The necessary and sufficient conditions for hygrothermal stability were derived in Cross et al. [4]. A summary is provided in the following for reference. The development begins with the constitutive relationship as given in classical lamination theory (CLT) [5]

$$\begin{Bmatrix} N_{xx} \\ N_{yy} \\ N_{xy} \\ M_{xx} \\ M_{yy} \\ M_{xy} \end{Bmatrix} = \begin{bmatrix} A_{11} & A_{12} & A_{16} & B_{11} & B_{12} & B_{16} \\ A_{12} & A_{22} & A_{26} & B_{12} & B_{22} & B_{26} \\ A_{16} & A_{26} & A_{66} & B_{16} & B_{26} & B_{66} \\ B_{11} & B_{12} & B_{16} & D_{11} & D_{12} & D_{16} \\ B_{12} & B_{22} & B_{26} & D_{12} & D_{22} & D_{26} \\ B_{16} & B_{26} & B_{66} & D_{16} & D_{26} & D_{66} \end{bmatrix} \begin{Bmatrix} \varepsilon_{xx} \\ \varepsilon_{yy} \\ \gamma_{xy} \\ \kappa_{xx} \\ \kappa_{yy} \\ \kappa_{xy} \end{Bmatrix} - \begin{Bmatrix} N_{xx} \\ N_{yy} \\ N_{xy} \\ M_{xx} \\ M_{yy} \\ M_{xy} \end{Bmatrix}^{(T,H)} \tag{2}$$

where N_{xx}, N_{yy}, N_{xy}, M_{xx}, M_{yy}, and M_{xy} are the stress resultants, and ε_{xx}, ε_{yy}, γ_{xy}, κ_{xx}, κ_{yy}, and κ_{xy} are the strains and curvatures. The stiffness coefficients are defined as

$$A_{ij} = \sum_{k=1}^{n} \bar{Q}_{ij(k)}(h_k - h_{k-1})$$

$$B_{ij} = \frac{1}{2}\sum_{k=1}^{n} \bar{Q}_{ij(k)}(h_k^2 - h_{k-1}^2)$$

$$D_{ij} = \frac{1}{3}\sum_{k=1}^{n} \bar{Q}_{ij(k)}(h_k^3 - h_{k-1}^3) \tag{3}$$

where $\bar{Q}_{ij(k)}$ and h_k represent the transformed reduced stiffness coefficients and height relative to the laminate midplane for the kth ply, respectively. The nonmechanical stress resultants are

$$\begin{Bmatrix} N_{xx} \\ N_{yy} \\ N_{xy} \end{Bmatrix}^{(T,H)} = (\Delta T, \Delta H) \sum_{k=1}^{n} [\bar{Q}]_k \{\bar{\alpha}, \bar{\beta}\}_k (h_k - h_{k-1}) \tag{4a}$$

$$\begin{Bmatrix} M_{xx} \\ M_{yy} \\ M_{xy} \end{Bmatrix}^{(T,H)} = \frac{1}{2}(\Delta T, \Delta H) \sum_{k=1}^{n} [\bar{Q}]_k \{\bar{\alpha}, \bar{\beta}\}_k (h_k^2 - h_{k-1}^2) \tag{4b}$$

where $\{\bar{\alpha}, \bar{\beta}\}_k$ are the transformed in-plane thermal and moisture expansion coefficients for the kth ply. The total number of plies in the laminate is n, and T and H denote thermal and hygral quantities, respectively.

By assuming each ply is an identical specially orthotropic lamina, it can be shown that $M_{xx}^{(T,H)} = -M_{yy}^{(T,H)}$. Because in this development to find hygrothermally stable laminates no mechanical stress resultants are being considered and hygrothermal stability requires zero out-of-plane curvatures, the constitutive law in Eq. (2) reduces to

$$\begin{Bmatrix} N_{xx} \\ N_{yy} \\ N_{xy} \\ M_{xx} \\ -M_{xx} \\ M_{xy} \end{Bmatrix}^{(T,H)} = \begin{bmatrix} A_{11} & A_{12} & A_{16} \\ A_{12} & A_{22} & A_{26} \\ A_{16} & A_{26} & A_{66} \\ B_{11} & B_{12} & B_{16} \\ B_{12} & B_{22} & B_{26} \\ B_{16} & B_{26} & B_{66} \end{bmatrix} \begin{Bmatrix} \varepsilon_{xx} \\ \varepsilon_{yy} \\ \gamma_{xy} \end{Bmatrix} \tag{5}$$

Solving this system generates two conditions, referred to subsequently as Condition A and Condition B. Both conditions together comprise the necessary and sufficient conditions for hygrothermal stability. Condition A is defined as having the two axial nonmechanical in-plane stress resultants equal and all other stress resultants zero, and Condition B is defined as having the coupling stiffness matrix identically equal to zero. Table 1 summarizes the necessary and sufficient conditions for hygrothermal stability and includes the sets of equations that satisfy these conditions. Note that using the last two equations from Condition A, it is possible to reduce the first two equations of Condition A to $\sum_{k=1}^{n} k\cos 2\theta_k = 0$ and $\sum_{k=1}^{n} k\sin 2\theta_k = 0$, respectively; this will not be adopted in the present work so as to remain consistent with the authors' development.

There are several elements worth noting with regard to these conditions. First, symmetric stacking sequences automatically satisfy Condition B, but can also satisfy Condition A; likewise, asymmetric stacking sequences can satisfy either Condition A or Condition B. Second, Condition B precludes the existence of any coupling between in-plane and out-of-plane deformation modes. Third, the conditions are material independent and are only functions of ply angle and the location of the ply in the stacking sequence. Therefore, any composite made from specially orthotropic plies will be hygrothermally stable if one of the conditions is met. An important benefit of this fact is that the hygrothermal stability of a laminate will not be influenced by variations in material properties.

Because Condition B precludes coupling between in-plane and out-of-plane deformation modes, a hygrothermally stable laminate with extension-twist coupling must have an asymmetric stacking sequence and meet the constraints of Condition A. Asymmetric laminates with fewer than five plies cannot satisfy Condition A [4]. There is only one unique five-ply laminate that is asymmetric and meets Condition A, given as [4]

$$[76.3/-33.6/0/33.6/-76.3] \tag{6}$$

The middle ply of the laminate was set to zero but could take any value. Rigidly rotated laminates will retain hygrothermal stability, but the magnitude of extension-twist coupling will vary.

III. Optimization Procedure

For laminates with more than five plies, expanding Condition A produces nontractable equations, and analytic solutions are not possible. Therefore, a constrained numerical optimization routine

Table 1 Necessary and sufficient conditions for hygrothermal stability

Condition A	OR	Condition B
Equal hygrothermal expansion in all directions and zero nonmechanical moment resultants, i.e., $N_{xx}^{(T,H)} = N_{yy}^{(T,H)}$ $N_{xy}^{(T,H)} = M_{xx}^{(T,H)} = M_{yy}^{(T,H)} = M_{xy}^{(T,H)} = 0$		Coupling stiffness matrix is zero, i.e., $B_{ij} = 0$
Satisfied when		Satisfied when
$\sum_{k=1}^{n}(2k-n-1)\cos 2\theta_k = 0$		$\sum_{k=1}^{n}(2k-n-1)\cos 2\theta_k = 0$
$\sum_{k=1}^{n}(2k-n-1)\sin 2\theta_k = 0$		$\sum_{k=1}^{n}(2k-n-1)\sin 2\theta_k = 0$
$\sum_{k=1}^{n}\cos 2\theta_k = 0$		$\sum_{k=1}^{n}(2k-n-1)\cos 4\theta_k = 0$
$\sum_{k=1}^{n}\sin 2\theta_k = 0$		$\sum_{k=1}^{n}(2k-n-1)\sin 4\theta_k = 0$

was used to identify hygrothermally stable stacking sequences that produce the maximum extension-twist coupling for a given number of plies. The constraints are the equations that satisfy Condition A, and the parameter that governs the level of extension-twist coupling is β_{16}, which can be determined by inverting Eq. (2), such that

$$\begin{Bmatrix} \varepsilon_{xx} \\ \varepsilon_{yy} \\ \gamma_{xy} \\ \kappa_{xx} \\ \kappa_{yy} \\ \kappa_{xy} \end{Bmatrix} = \begin{bmatrix} \alpha_{11} & \alpha_{12} & \alpha_{16} & \beta_{11} & \beta_{12} & \beta_{16} \\ \alpha_{12} & \alpha_{22} & \alpha_{26} & \beta_{21} & \beta_{22} & \beta_{26} \\ \alpha_{16} & \alpha_{26} & \alpha_{66} & \beta_{61} & \beta_{62} & \beta_{66} \\ \beta_{11} & \beta_{21} & \beta_{61} & \delta_{11} & \delta_{12} & \delta_{16} \\ \beta_{12} & \beta_{22} & \beta_{62} & \delta_{12} & \delta_{22} & \delta_{26} \\ \beta_{16} & \beta_{26} & \beta_{66} & \delta_{16} & \delta_{26} & \delta_{66} \end{bmatrix} \begin{Bmatrix} N_{xx} \\ N_{yy} \\ N_{xy} \\ M_{xx} \\ M_{yy} \\ M_{xy} \end{Bmatrix} + \begin{Bmatrix} \varepsilon_{xx} \\ \varepsilon_{yy} \\ \gamma_{xy} \\ \kappa_{xx} \\ \kappa_{yy} \\ \kappa_{xy} \end{Bmatrix}^{(T,H)} \tag{7}$$

Because extension-twist coupling assumes that only an axial stress is applied and the resulting twist rate is of interest, the relationship between these two quantities taking into account hygrothermal stability is

$$\varphi = \frac{\kappa_{xy}}{2} = \frac{\beta_{16} N_{xx}}{2} = \frac{1}{2}(nt\beta_{16}\sigma_{xx}) \tag{8}$$

Table 2 Material properties of graphite/epoxy T300/976

E_{11}	125 GPa
E_{22}	8.45 GPa
G_{12}	4.3 GPa
ν_{12}	0.328
t	0.152 mm

where n, t, and σ_{xx} are the number of plies, the thickness of each ply, and the applied axial stress, respectively.

The sequential quadratic programming (SQP) [6] implementation in MATLAB^{TM} [7] was used to perform the numerical optimization. SQP is a gradient-based method that minimizes an objective function while meeting constraint conditions. Because the optimizer minimizes the objective function, the function was chosen to be $-\beta_{16}^2$. Using equations from CLT, the objective and constraint functions were programmed for any given stacking sequence. The objective function returned the values of $-\beta_{16}^2$ while the constraint function returned the vector

$$\begin{Bmatrix} \sum_{k=1}^{n}(2k-n-1)\cos 2\theta_k \\ \sum_{k=1}^{n}(2k-n-1)\sin 2\theta_k \\ \sum_{k=1}^{n}\cos 2\theta_k \\ \sum_{k=1}^{n}\sin 2\theta_k \end{Bmatrix} \tag{9}$$

The `fmincon` function was used, with inputs of the objective function, a randomly selected initialization stacking sequence, and the constraints as given in Eq. (9). The initialization stacking sequence consisted of randomly chosen ply angles from the range $[-90, 90°]$. The output of the optimizer was the optimal stacking sequence and value of the objective function for that stacking sequence.

Although the hygrothermal stability conditions are material independent, the magnitude of extension-twist coupling is not. Therefore, the properties of a T300/976 graphite/epoxy material system, used to manufacture the specimens, were chosen for the optimization. These properties are provided in Table 2 as measured in accordance with American Society for Testing and Materials (ASTM) standards [8,9]. The thickness of a ply was found by measuring the laminate thickness with a Vernier caliper and dividing that by the number of plies.

The optimization was performed for five- through ten-ply laminates, as well as the Winckler-type laminate for comparison. Because of the existence of many suboptimal extrema and the gradient-based method's tendency to converge to local optima, several hundred optimizations were performed with different initialization stacking sequences to provide confidence in the global optima. The results of the optimizations are provided in Table 3. To compare the amount of extension-twist coupling, a nondimensional parameter is introduced, given as

Table 3 Extension-twist optimized hygrothermally stable stacking sequences

Laminate	Stacking sequence, °	β_{16}, N^{-1}	η	Percent increase in coupling over Winckler
5-ply	$[-58.7/11.4/45/78.6/-31.3]$	$2.00 \cdot 10^{-4}$	1759	81.0%
6-ply	$[21.2/-63.8/-48.7/48.7/63.8/-21.2]$	$1.82 \cdot 10^{-4}$	1927	98.5%
7-ply	$[14.1/-76.9/-73.9/45/-16.1/-13.2/75.7]$	$1.15 \cdot 10^{-4}$	1423	46.5%
8-ply	$[-21.5/72.1/57.9/-29.6/29.6/-57.9/-72.1/21.5]$	$8.99 \cdot 10^{-5}$	1264	30.2%
9-ply	$[25.5/-79/32.5/-62.9/49.9/27.4/57/-10.6/64.9]$	$7.98 \cdot 10^{-5}$	1254	29.1%
10-ply	$[16.2/-69.0/-65.3/31.8/42.1/-42.1/-31.8/65.3/69.0/-16.2]$	$7.09 \cdot 10^{-5}$	1245	28.2%
Winckler	$[22.5/-67.5_2/22.5/-22.5/67.5_2/-22.5]$	$7.56 \cdot 10^{-5}$	971	-

Table 4 Global and angle-ply optimal lay ups with constrained optima percent loss

Laminate	Unconstrained, °	Angle-ply, °	Angle-ply % loss	Hygrothermally stable % loss
2-ply	$[\pm 24.7]$	$[\pm 24.7]$	0.0%	N/A
3-ply	$[-30.1/90/30.1]$	$[-30.1/90/30.1]$	0.0%	N/A
4-ply	$[28.5/-89.5]_A$	$[\pm(24.7_2)]$	47.8%	N/A
5-ply	$[-27.6/90_3/27.6]$	$[30.9_2/90/-30.9_2]$	24.8%	51.9%
6-ply	$[-26.1/-38.6/88.6]_A$	$[\pm(24.7_3)]$	49.5%	37.2%
7-ply	$[-25.8/-35.4/89.6/\overline{90}]_A$	$[30.6_3/90/-30.6_3]$	33.1%	47.0%
8-ply	$[-25.6/-33.4/89.9/89.8]_A$	$[\pm(24.7_4)]$	50.7%	46.5%
9-ply	$[24.8/31.3/42.0/-89.2/\overline{90}]_A$	$[30.0_4/90/-30.0_4]$	37.4%	40.5%
10-ply	$[24.7/30.4/39.0/-89.5/-89.1]_A$	$[\pm(24.7_5)]$	51.2%	34.8%

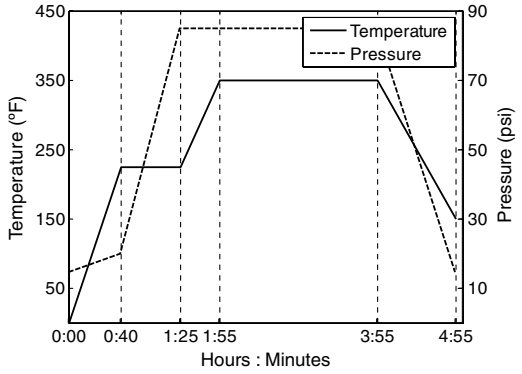

Fig. 1 Curing cycle for graphite/epoxy material system.

$$\eta = \left|\frac{1}{2} ntLE_{11}\beta_{16}\right| = \frac{\varphi LE_{11}}{\sigma_o} \approx \frac{\theta_t}{\varepsilon_{11}} \tag{10}$$

which is approximately proportional to the twist per unit nominal strain applied to a narrow strip of the laminate. E_{11} and t are the elastic modulus along the fiber direction and the thickness of a ply, respectively, as given in Table 2, n is the number of plies, ε_{11} and σ_o are the nominal axial strain and stress, respectively, and θ_t is the twist angle. Several trends are worth noting. First, the five-ply laminate is a rigid rotation of Eq. (6), as expected. Second, the coupling tends to decrease with an increase in the number of plies; this is due to the increase in the axial torsional stiffness associated with thicker laminates. Third, the optimal even-ply laminates are antisymmetric, while the optimal odd-ply laminates are nearly 45° rotations of antisymmetric stacking sequences.

Because angle-ply laminates are the most intuitive solution to extension-twist coupling, angle-ply and unconstrained laminates were optimized for extension-twist coupling to compare with optimal hygrothermally stable laminates. The results are shown in Table 4, where a subscript A indicates an antisymmetric stacking sequence. Parameter η was calculated for each laminate, and the percent loss in coupling relative to the unconstrained maxima was calculated for every optimal angle-ply and hygrothermally stable laminate, calculated as

$$\text{Percent Loss} = (\eta_{um} - \eta_{cm}) \times 100/\eta_{um} \tag{11}$$

where η_{um} and η_{cm} correspond to the maximum η of the unconstrained and constrained laminates. These comparisons will help determine if a coupled system should be redesigned. For example, if a six-ply angle-ply laminate is being used to achieve extension-twist coupling, a 12.3% increase in coupling are achievable with a hygrothermally stable laminate, calculated as 49.5% − 37.2% from Table 4.

IV. Testing and Verification

Several methods of verification were used to confirm the level of coupling predicted by the optimizer, including manufacture and testing, a nonlinear analytical model, and finite element analysis. Each of the laminates in Table 3 were manufactured as panels from T300/976 graphite/epoxy material system with properties given in Table 2, laid up in a flat mold, and cured in an autoclave with the curing cycle shown in Fig. 1 and dimensions 0.41 by 0.31 m (16 by 12"). Five specimens were cut from the central region of each laminated panel with dimensions of 2.54 by 25.4 cm (1.0 by 10.0") adopted from the test method for tensile properties, ASTM Standard D 3039 [8]. Fiberglass tabs of dimensions 2.54 by 3.81 cm (1.0 by 1.5") were manufactured and attached at both ends and on both sides of each specimen, leaving test sample dimensions of 2.54 by 17.8 cm (1.0 by 7.0"). One of each of the 6-ply and Winckler-type specimens and two of the 7-ply specimens were damaged prior testing. The optimal Winckler-type laminate is being used as reference to compare the levels of coupling achieved by the optimal laminates. Laminate thickness was measured with a Vernier caliper, and ply thickness was found to be consistent with that found during material characterization as given in Table 2.

The specimens were tested in an Instron 8874 biaxial tension-torsion machine. The displacement control mode was used to measure tip twist, and the load control mode was used to apply axial force. For each specimen, the tip pretwist was measured by setting the axial load to zero. In all cases the pretwist was small, as expected from a flat hygrothermally stable laminate. Table 5 includes the measured pretwist values and specimen ply thickness t and width w. Axial force was subsequently applied in increments of 445 N (100 lb) up to 2224 N (500 lb). For each loading the specimen tip was rotated until the torque in the system read zero, and the tip rotation angle was recorded. The tip twist angle was adjusted manually due to the relatively low torsional stiffness of the specimens compared with the capacity of the torque load cell. This process was repeated to acquire all axial-force/tip twist data points. The specimens did not exhibit any hysteresis upon loading and unloading.

The data are plotted in Figs. 2–8 for each of the laminates in Table 3. Also included for verification are finite element analysis results and a geometrically nonlinear model [10], given by

$$F_a = \frac{(b_1 + \frac{4}{3}b_2\varphi_{oL} + 2b_3\varphi_{oL}^2)\varphi_L}{[b_4 - (\varphi_L + \varphi_{oL})]} \tag{12}$$

where F_a is axial force, ϕ_{oL} is the tip pretwist angle, ϕ_L is the tip twist angle, and b_1–b_4 are functions of the geometric parameters and stiffness coefficients, defined as

$$b_1 = \frac{8\psi k_1}{b\alpha_{11}k_3} \tag{13a}$$

Table 5 Pretwist and measured thickness and width for manufactured specimens

Specimen	Pretwist, °	t, mm	w, cm
5-ply #1	1.4	0.147	2.52
5-ply #2	1.2	0.147	2.57
5-ply #3	1.5	0.147	2.55
5-ply #4	1.7	0.152	2.55
5-ply #5	0.0	0.147	2.54
6-ply #1	−1.9	0.165	2.73
6-ply #2	−2.0	0.173	2.62
6-ply #3	−4.1	0.161	2.72
6-ply #4	−3.7	0.156	2.68
6-ply #5		(damaged)	
7-ply #1		(damaged)	
7-ply #2	−0.8	0.167	2.67
7-ply #3	0.8	0.167	2.70
7-ply #4	1.0	0.167	2.72
7-ply #5		(damaged)	
8-ply #1	−1.4	0.156	2.58
8-ply #2	−1.3	0.152	2.59
8-ply #3	−0.7	0.149	2.60
8-ply #4	−1.7	0.152	2.57
8-ply #5	−1.1	0.149	2.57
9-ply #1	0.8	0.152	2.51
9-ply #2	0.0	0.153	2.55
9-ply #3	0.4	0.152	2.52
9-ply #4	1.0	0.152	2.54
9-ply #5	1.5	0.152	2.52
10-ply #1	−2.3	0.150	2.72
10-ply #2	−2.1	0.152	2.62
10-ply #3	−2.2	0.152	2.48
10-ply #4	−2.1	0.152	2.48
10-ply #5	−1.8	0.152	2.48
Winckler #1	0.1	0.152	2.67
Winckler #2	0.3	0.152	2.70
Winckler #3	0.7	0.152	2.66
Winckler #4	0.2	0.156	2.66
Winckler #5		(damaged)	

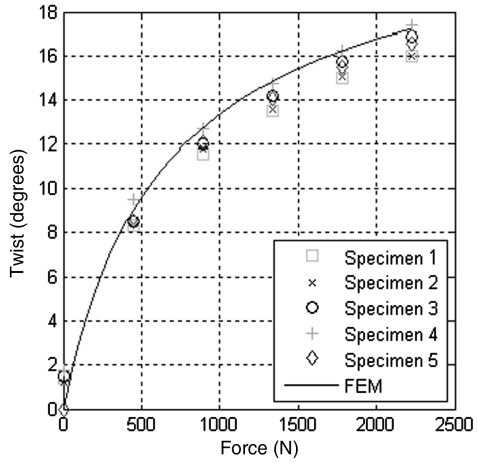

Fig. 2 Optimal five-ply laminate, given by [−58.7/11.4/45/78.6/−31.3].

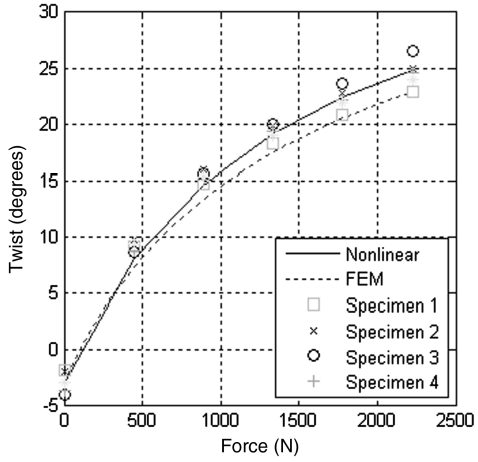

Fig. 3 Optimal six-ply laminate, given by [21.2/ − 63.8/ − 48.7/48.7/63.8/ − 21.2].

$$b_2 = -\frac{2b\alpha_{12}}{L}(1+2\rho)(k_1 + k_2 k_4) \tag{13b}$$

$$b_3 = \frac{\rho\alpha_{11}b^3}{L^2}\left(k_4\left(k_3 - \frac{2}{15} - \frac{2\alpha_{12}^2 k_2}{\alpha_{11}\beta b^2}\right) - k_3\right) \tag{13c}$$

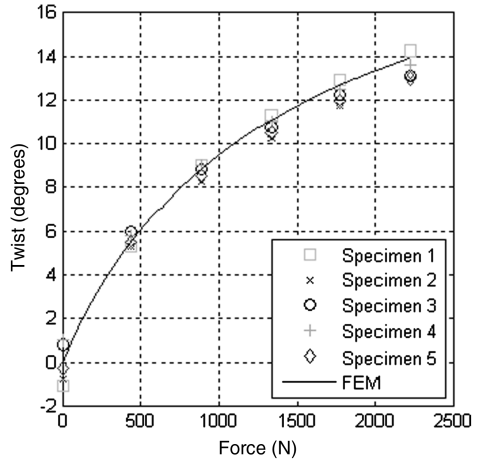

Fig. 4 Optimal seven-ply laminate, given by [14.1/ − 76.9/ − 73.9/45/ − 16.1/ − 13.2/75.7].

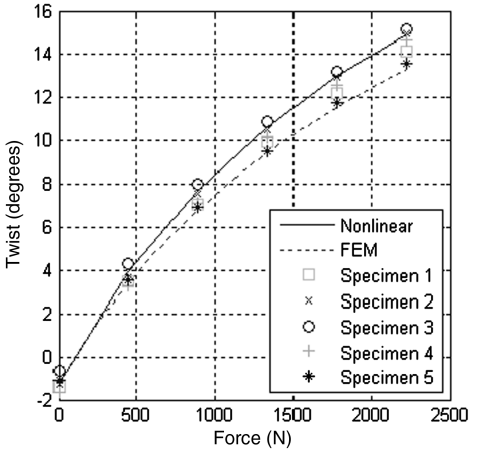

Fig. 5 Optimal eight-ply laminate, given by [−21.5/72.1/57.9/−29.6/29.6/ − 57.9/ − 72.1/21.5].

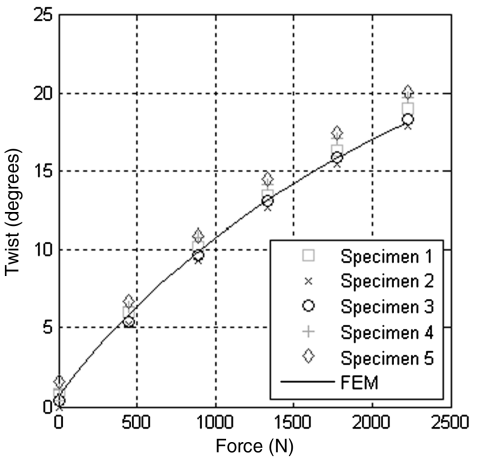

Fig. 6 Optimal nine-ply laminate, given by [25.5/ − 79/32.5/−62.9/49.9/27.4/57/ − 10.6/64.9].

$$b_4 = -\frac{2\alpha_{12}k_1 L}{\alpha_{11}k_3 b^2} \tag{13d}$$

where L and b are the length and half-width of the specimen ρ is a tracer introduced to isolate the contribution of the axial force to the twisting moment ($\rho = 0$ removes the effect of the axial force and $\rho = 1$ includes the effect of the axial force), and

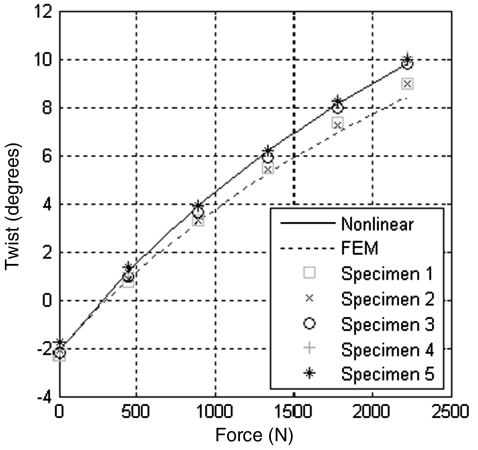

Fig. 7 Optimal ten-ply laminate, given by [16.2/ − 69.0/ − 65.3/31.8/42.1/ − 42.1/ − 31.8/65.3/69.0/ − 16.2].

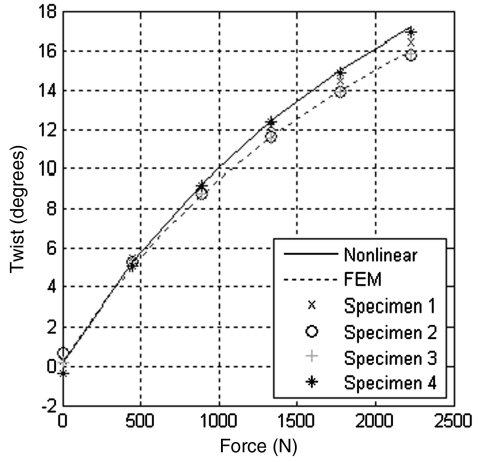

Fig. 8 Optimal Winckler-type laminate, given by $[22.5/-67.5_2/22.5/-22.5/67.5_2/-22.5]$.

$$k_1 = 1 - \frac{\tanh(bs)}{bs} \tag{14a}$$

$$k_2 = \frac{2}{3} - k_1\left(1 + \frac{2}{(sb)^2}\right) \tag{14b}$$

$$k_3 = \frac{1}{3} - \frac{\alpha_{12}^2}{\alpha_{11}\alpha_{22}}\left(\frac{1}{3} + k_2\right) \tag{14c}$$

$$k_4 = \frac{\psi + \alpha_{12}^2 k_1}{\alpha_{11}\alpha_{22}k_3} \tag{14d}$$

and

$$\psi = \alpha_{11}\alpha_{22} - \alpha_{12}^2 \tag{15a}$$

$$s = \sqrt{\frac{\beta}{\alpha_{22}}} \tag{15b}$$

and

$$\alpha_{11} = A_{11} - \frac{A_{12}^2}{A_{22}} \tag{16a}$$

$$\alpha_{22} = D_{66} - \frac{B_{26}^2}{A_{22}} \tag{16b}$$

$$\alpha_{12} = B_{16} - \frac{A_{12}B_{26}}{A_{22}} \tag{16c}$$

$$\beta = A_{55} - \frac{A_{45}^2}{A_{44}} \tag{16d}$$

where the stiffness coefficients are given in Eq. (3). The nonlinear model was developed by assuming finite rigid rotation of the cross sections and including a St. Venant-type warping where out-of-plane shear and transverse normal strains are neglected. It is valid for antisymmetric laminates with $h \ll w \ll L$; therefore, predictions are only included for even-ply optimal extension-twist laminates. Geometric nonlinearity is associated with the finite twist rotations.

Finite element analysis was performed in ABAQUS™ 6.8-1. Laminates were created to the same dimensions and stacking sequences as the manufactured specimens. Specimen thickness was calculated from the total thickness of the manufactured laminates. An 8-node, doubly curved, thin-shell, reduced-integration element type was selected with 5 degrees of freedom per node (S8R5), and 38 elements were used along the length and 5 elements across the width; a schematic of a representative mesh is given in Fig. 9. One end of the model was clamped, and a shell edge load was applied such that the total axial force was ramped up to 2224 N (500 lb). Geometrically nonlinear formulation was selected and the transverse deflection of the tip corners was extracted as a function of load and used to calculate the twist angle. There is good agreement between the finite element (FEM) predictions and test data. The nonlinear model assumes pure twist and is stiffer compared with FEM predictions.

V. Discussion of Results

A summary of the test data is presented in Figs. 10 and 11 with error bars showing maximum and minimum values from all laminates along with the FEM predictions. The tip twist is divided by the specimen length to allow for comparison of twist rate among laminates. The twist rate is shown as a function of load and stress in Figs. 10 and 11, respectively. The stress is calculated by dividing the force by the average area of each specimen for a given laminate based on measured values for the thickness and width. The pretwist is subtracted from all test data so that the curve for each laminate begins at the origin.

As predicted by the performance parameter, nearly all of the tested laminates outperform the previously known Winckler-type laminate. For example, when compared at a load level of 2224 N, the six-ply laminate, with $\eta = 1927$, outperforms the Winckler-type laminate, with $\eta = 971$, by 59%. This is accompanied by a 25% weight savings. Even the ten-ply laminate, which has a 25% thickness penalty and $\eta = 1245$, outperforms the Winckler-type laminate by 26% at the same loading. The seven-ply laminate is the only laminate that does not outperform the Winckler-type laminate at loads between 1200 and 2224 N.

When compared at the same axial force, the coupling tends to decrease as the number of plies increases. This follows the same trend as the performance parameter given in Table 3 and the same reasoning applies; as the laminates become thicker, the axial and torsional stiffnesses become greater. Laminates with an even number of plies tend to outperform those with an odd number of plies. One likely explanation is that when going from an even-ply to an odd-ply

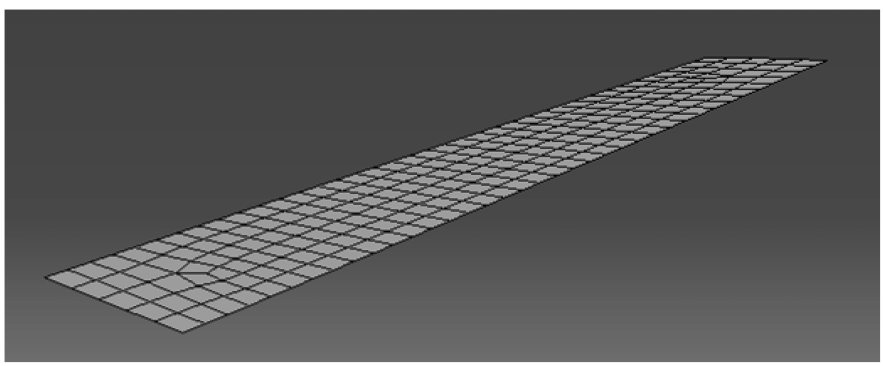

Fig. 9 Representative FEM.

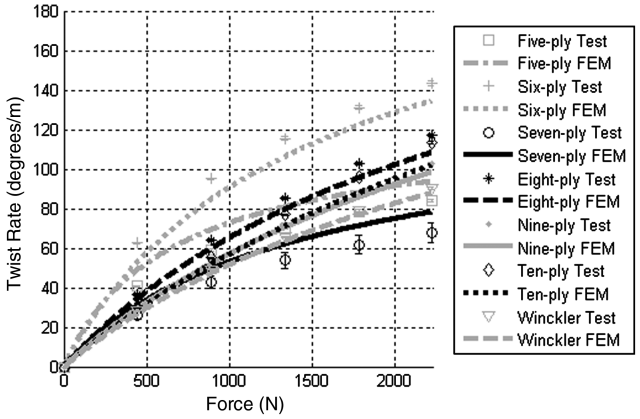

Fig. 10 Comparison of optimal extension-twist laminates by force.

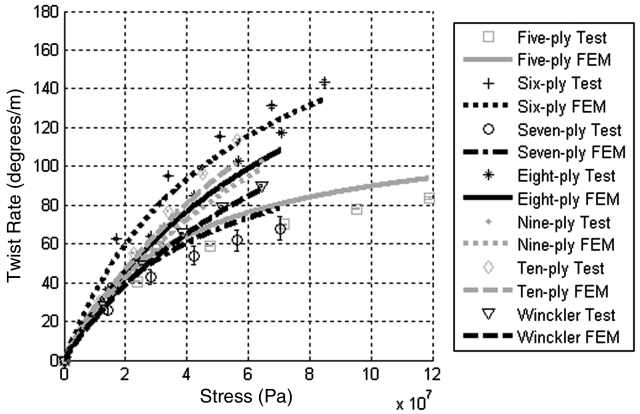

Fig. 11 Comparison of optimal extension-twist coupling by stress.

laminate, the addition of a ply along the midplane increases the axial and torsional stiffnesses more than the coupling. For this reason, odd-ply laminates make suboptimal choices for extension-twist coupling.

Geometric nonlinearity associated with finite twisting rotations is quite apparent in Figs. 10 and 11. A general trend shows that for laminates with fewer plies, the nonlinear behavior is more pronounced, while for laminates with a greater number of plies, the coupling response is closer to linear. The five-ply laminate demonstrates this effect best: at a low loading, it produces one of the highest twist rates, but by 2224 N, it has the one of the lowest twist rates. This phenomenon can be explained by noting that the finite

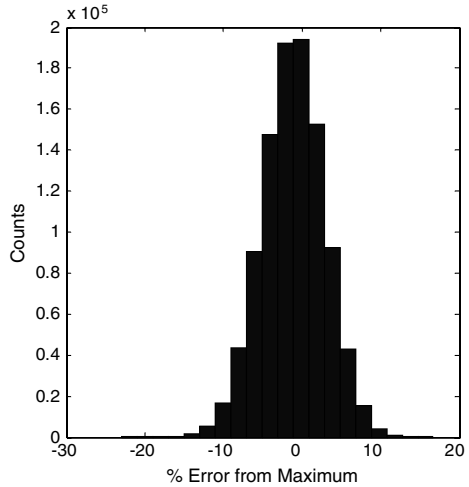

Fig. 12 Robustness of the optimal hygrothermally stable six-ply laminate.

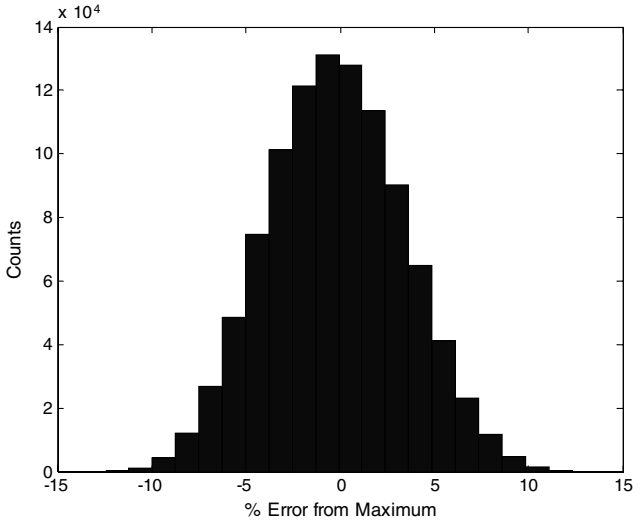

Fig. 13 Robustness of the optimal angle-ply six-ply laminate.

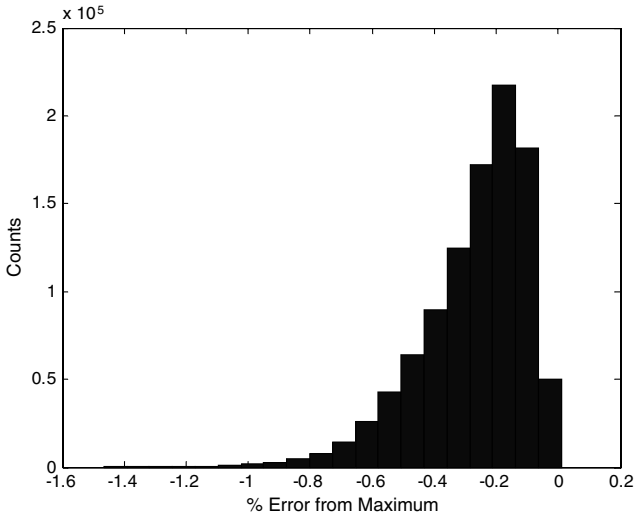

Fig. 14 Robustness of globally optimal six-ply laminate.

twist arises largely due to the small ratio of torsional to extensional stiffness exhibited by extension-twist coupled laminates [10]; this ratio is, for example, approximately 4 times larger in the ten-ply laminate as compared with the five-ply laminate, which explains why the five-ply laminate exhibits more nonlinearity than the ten-ply laminate.

Comparing optimized laminates at the same stress level allows for some of the effect of torsional stiffness to be factored out. At a stress level of 5.65×10^7 Pa, which is the greatest stress experienced by the ten-ply laminate, the six-ply laminate, with $\varphi = 112°/\text{m}$, exhibits the highest twist rate, an increase of 38.2% over the Winckler-type laminate, with $\varphi = 81.3°/\text{m}$. The laminate with the next-most coupling is the ten-ply laminate, with $\varphi = 102°/\text{m}$, which has an increase in coupling of 29.0% over the Winckler laminate. One possible explanation for the ten-ply laminate's coupling to be so high at the same stress is because the outermost plies of the ten-ply laminate are farther from the midplane than those of the eight-ply laminate, causing the extension-shear coupling in these plies to induce a larger torsional moment.

VI. Robustness

For extension-twist coupled laminates to be useful, small errors in ply angle cannot cause significant loss of coupling. Therefore, a study was conducted to investigate the sensitivity of a representative

laminate to small errors in ply angle. The optimal six-ply stacking sequences were chosen for this study. To model manufacturing errors within a given laminate, a set of 10^6 perturbed stacking sequences was generated by randomly selecting each ply angle from the interval $[\theta_k \mp 2^\circ]$, where θ_k is the fiber-orientation angle of the kth ply in the optimal stacking sequence; this distribution is assumed to be typical of hand-layup manufacturing errors.

The error between the perturbed and optimal laminate's performance parameter was calculated as

$$\text{Percent Error} = (\eta_p - \eta_o) \times 100/\eta_o \tag{17}$$

where η_p and η_o corresponding to the η of the perturbed and optimal laminates. Histograms presenting the results of the study are given in Figs. 12–14 for the hygrothermally stable, angle-ply and globally optimal laminates, respectively. The error is mostly contained to within $\pm 10\%$ of the expected coupling for the hygrothermally stable and angle-ply laminates. It should be noted that the error can be positive even though the stacking sequence yields maximum coupling because lay-ups with perturbed ply angles are not subject to the constraints of the baseline laminate. For example, perturbed laminates in Fig. 12 may not be strictly hygrothermally stable. The error of the globally optimal laminates is contained within 1%.

VII. Conclusions

The necessary and sufficient conditions for hygrothermal stability are a combined set of conditions that entail having either the out-of-plane moments and in-plane shear force equal to zero along with both in-plane axial forces equal to each other or the coupling stiffness matrix equal to zero. From within these conditions, stacking sequences that maximize extension-twist coupling have been found for laminates consisting of five through ten plies. Analytical predictions confirmed by test data show that this new class of optimum laminates outperforms Winckler-type stacking sequences. An investigation of hygrothermally stable laminates with a range of couplings, including bending-twist and combined extension and bending-twist, is underway.

Acknowledgments

The authors gratefully acknowledge the support given by the National Defense Science and Engineering Graduate Fellowship and the University of Texas System STARS Program.

References

[1] Hyer, M. W., "Some Observations on the Curved Shape of Thin Unsymmetric Laminates," *Journal of Composite Materials*, Vol. 15, No. 2, 1981, pp. 175–194. doi:10.1177/002199838101500207

[2] Hyer, M. W., "The Room-temperature Shapes of Four-layer Unsymmetric Cross-ply Laminates," *Journal of Composite Materials*, Vol. 16, No. 4, 1982, pp. 318–340. doi:10.1177/002199838201600406

[3] Winckler, S. I., "Hygrothermally Curvature Stable Laminates with Tension-torsion Coupling," *Journal of the American Helicopter Society*, Vol. 30, No. 3, 1985, pp. 56–58. doi:10.4050/JAHS.30.56

[4] Cross, R. J., Haynes, R. A., and Armanios, E. A., "Families of Hygrothermally Stable Asymmetric Laminated Composites," *Journal of Composite Materials*, Vol. 42, No. 7, 2008, pp. 697–716. doi:10.1177/0021998308088597

[5] Jones, R. M., *Mechanics of Composite Materials*, 2nd ed., Taylor & Francis, Philadelphia, PA, 1999, pp. 190–203.

[6] Gill, P. E., Murray, W., and Wright, M. H., *Practical Optimization*, Academic Press, London, UK, 1981.

[7] The MathWorks, Inc., MATLAB [CD-ROM], Version 7.2.0.232 (R2006a), Natick, MA., 2006.

[8] American Society for Testing and Materials, Standard Test Method for Tensile Properties of Polymer Matrix Composite Materials, ASTM Standard D 3039/D 3039M, ASTM International, 2006.

[9] American Society for Testing and Materials, Standard Test Method for In-Plane Shear Response of Polymer Matrix Composite Materials by Tensile Test of a $\pm 45^\circ$ Laminate, ASTM Standard D 3518/D 3518M, ASTM International, 2001.

[10] Armanios, E. A., Makeev, A., and Hooke, D., "Finite-Displacement Analysis of Laminated Composite Strips with Extension-Twist Coupling," *Journal of Aerospace Engineering*, Vol. 9, No. 3, 1996, pp. 80–91. doi:10.1061/(ASCE)0893-1321(1996)9:3(80)

M. Hyer
Associate Editor